

CHAPTER 7

FAILURE CRITERIA OF SHAFT MATERIAL

7.1 INTRODUCTION

Deformations in any structural element depend upon the characteristics of the load, the element shape and its material properties. With laterally loaded shafts and shafts, the flexural deformations are based on the applied moment and the flexural stiffness of the shaft at the cross section in question. In addition, the flexural stiffness (EI) of the shaft is a function of the Young's modulus (E), moment of inertia (I) of the shaft cross section and the properties of the surrounding soil. Given the type of material, concrete and/or steel, the properties of shaft material vary according to the level of the applied stresses.

Behavior of shafts under lateral loading is basically influenced by the properties of both the soil and shaft (shaft material and shape). The nonlinear modeling of shaft material, whether it is steel and/or concrete, should be employed in order to predict the value of the lateral load and the realistic associated bending moment and shaft deflection especially at large values of shaft-head deflection and the onset of shaft material failure. It is known that the variation in the bending stiffness (EI) of a laterally loaded shaft is a function of the bending moment distribution along the shaft (moment-curvature, $M-\Phi$, relationship) as seen in Fig. 7-1.

Consequently, some of the shaft cross sections which are subjected to high bending moment experience a reduction in bending stiffness and softer interaction with the surrounding soil. Such behavior is observed with drilled shafts and steel shafts at advanced levels of loading and has an impact on the lateral response and capacity of the loaded shaft. The shaft bending stiffnesses along the deflected shaft change with the level of loading, the $M-\Phi$ relationship of the shaft material, and the soil reaction which affects the pattern of shaft deflection. Therefore, the equilibrium among the distributions of shaft deflection, bending moment, bending stiffness, and soil reaction along the shaft should be maintained.

In the case of a steel shaft, the Young's modulus remains constant (elastic zone) until reaching the yield stress, f_y (indicating the initial yielding), at which time the steel starts to behave elastic-plastically with different values of the secant Young's modulus. Once a plastic hinge develops, the shaft cross section responds in plastic fashion under a constant plastic moment. But, in the case of a concrete shaft, the stress-strain relationship varies in a nonlinear fashion producing a simultaneous reduction in Young's modulus and, in turn, the stiffness of the shaft cross section. Furthermore, once it reaches a critical value of strain, the concrete ruptures catastrophically.

The technique suggested by Reese (1984), which employs the Matlock-Reese p-y curves, requires separate evaluation of the $M-\Phi$ relationship of the shaft cross section and then adoption of a reduced bending stiffness (EI_r) to replace the original shaft bending stiffness (EI). The suggested procedure utilizes this reduced bending stiffness (EI_r) over the full length of the shaft at all levels of loading. Assuming a reasonable reduction in bending stiffness, particularly with drilled shafts, is a critical matter that requires guidance from the literature which has only limited experimental data. At the same time, the use of one constant reduced bending stiffness for the shaft does not reflect the real progressive deformations and forces associated with the steps of lateral loading. However, this technique may work quite well with the steel H-pile which fails approximately once the shaft flange reaches the yielding stage (occurs rapidly). In general, the response of the shaft (shaft-head load vs. deflection, and shaft-head load vs. maximum moment) is assessed based on a constant bending stiffness (EI) and is truncated at the ultimate bending moment of the original shaft/drilled shaft cross section. The moment-curvature relationship, and thus the maximum bending moment carried by the shaft cross section should be evaluated first.

Reese and Wang (1994) enhanced the technique presented above by computing the bending moment distribution along the shaft and the associated value of EI at each increment of loading. Reese and Wang (1994) concluded that the bending moment along the shaft does not depend strongly on structural characteristics and that the moment differences due to EI variations are small. It should be noted that the effect of the varying EI on the bending moment values along the drilled shaft was not obvious because the

EI of the drilled shaft had no effect on the p-y curves (i.e. modulus of subgrade reaction) employed in their procedure. Therefore, it was recommended that a single value of EI of the cracked section (constant value) be used for the upper portion of the shaft throughout the analysis. Contrary to Reese and Wang's assumption, the variation in the value of EI has a significant effect on the nature of the p-y curve and modulus of subgrade reaction [Ashour and Norris (2000); Yoshida and Yoshinaka (1972); and Vesic (1961)] especially in the case of large diameter shafts.

The main purpose in this chapter is to assess the moment-curvature relationship ($M-\phi$) of the loaded shaft in a convenient and simplified fashion considering the soil-shaft interaction. The prediction of the moment-curvature curve allows one to realistically determine the variation of shaft stiffness (EI) as a function of bending moment.

The SW model allows the designer to include the nonlinear behavior of the shaft material and, as a result, to find out the effect of material types on the shaft response and its ultimate capacity based on the concepts of soil-shaft interaction.

7.2 COMBINATION OF MATERIAL MODELING WITH THE STRAIN WEDGE MODEL

The bending moment distribution along the deflected length of a laterally loaded shaft varies as shown in Fig. 7-1. This profile of moment indicates the associated variation of shaft stiffness with depth if the stress-strain relationship of shaft material is nonlinear. The strain wedge model is capable of handling the nonlinear behavior of shaft material as well as the surrounding soil. The multi-sublayer technique, presented in Chapter 5, allows one to provide an independent description for each soil sublayer and the associated shaft segment. The effect of shaft material is considered with the global stability of the loaded shaft and the shape of the developing passive wedge of soil in front of the shaft. During the iteration process using the SW model, the stiffness of each shaft segment, which has a length equal to the depth of the soil sublayer, is a function of the calculated bending moment at the associated shaft segment, as seen in Fig. 7-1. Therefore,

the shaft is divided into a number of segments of different values of flexural stiffness under a particular lateral load.

In order to incorporate the effect of material non-linearity, numerical material models should be employed with the SW model. A unified stress-strain approach for confined concrete has been employed with the reinforced concrete shaft as well as the steel pipe shaft filled with concrete. In addition, steel is modeled using an elastic perfectly plastic uniaxial stress-strain relationship which is commonly used to describe steel behavior. The procedure presented provides the implementation of soil-shaft interaction in a fashion more sophisticated than that followed in the linear analysis with the SW model presented in Chapter 5.

The approach developed will allow one to load the shaft to its actual ultimate capacity for the desired lateral load and bending moment according to the variation of shaft material properties along the shaft length.

7.2.1 Material Modeling of Concrete Strength and Failure Criteria

Based upon a unified stress-strain approach for the confined concrete proposed by Mander et al. (1984 and 1988), a concrete model is employed with circular and rectangular concrete sections. The proposed model, which is shown in Fig. 7-2, has been employed for a slow strain rate and monotonic loading. The longitudinal compressive concrete stress f_c is given by

$$f_c = \frac{f_{cc} x r}{r - 1 + x^r} \quad (7-1)$$

where f_{cc} symbolizes the compressive strength of confined concrete.

$$x = \frac{\mathbf{e}_c}{\mathbf{e}_{cc}} \quad (7-2)$$

where ϵ_c indicates the axial compressive strain of concrete.

$$\mathbf{e}_{cc} = \mathbf{e}_{co} \left[1 + 5 \left(\frac{f_{cc}}{f_{co}} - 1 \right) \right] \quad (7-3)$$

where ϵ_{cc} is the axial strain at the peak stress. f_{co} and ϵ_{co} represent the unconfined (uniaxial) concrete strength and the corresponding strain, respectively. Generally, ϵ_{co} can be assumed equal to 0.002, and

$$r = \frac{E_c}{E_c - E_{sec}} \quad (7-4)$$

where

$$E_c = 57,000 (f_{co})^{0.5} \quad (p s i) \quad (7-5)$$

and

$$E_{\text{sec}} = \frac{f_{cc}}{e_{cc}} \quad (7-6)$$

E_c denotes the initial modulus of elasticity of the concrete under slowly applied compression load.

As mentioned by Paulay and Priestly (1992), the strain at peak stress given by Eqn. 7-3 does not represent the maximum useful strain for design purposes. The concrete strain limits occur when transverse confining steel fractures. A conservative estimate for ultimate compression strain (ϵ_{cu}) is given by

$$e_{cu} = 0.004 + \frac{1.4 r_s f_{yh} e_{sm}}{f_{cc}} \quad (7-7)$$

where ϵ_{sm} is the steel strain at maximum tensile stress (ranges from 0.1 to 0.15), and ρ_s is the volumetric ratio of confining steel. Typical values for ϵ_{cu} range from 0.012 to 0.05. f_{yh} represents the yield stress of the transverse reinforcement.

In order to determine the compressive strength of the confined concrete (f_{cc}), a constitutive model (Mander et al. 1988) is directly related to the effective confining stress (f_l) that can be developed at the yield of the transverse reinforcement.

$$f_{cc} = f_{co} \left[-1.254 + 2.254 \left(1 + \frac{7.94 f_l}{f_{co}} \right)^{0.5} - \frac{2 f_l}{f_{co}} \right] \quad (7-8)$$

For circular and square section of concrete, f_t is given by

$$f_t = 0.95 r_s f_{yh} \quad (7-9)$$

- **Monotonic tensile loading**

Although concrete tension strength is ignored in flexural strength calculation, due to the effect of concrete confinement it would be more realistic if it were considered in the calculation. As suggested by Mander et al. (1988), a linear stress-strain relationship is assumed in tension up to the tensile strength (f_{tu}). The tensile stress is given by

$$f_t = E_c e_c \quad \text{for } f_t \leq f_{tu} \quad (7-10)$$

and

$$e_{tu} = \frac{f_{tu}}{E_c} \quad (7-11)$$

where

$$f_{tu} = 9 (f_{co})^{0.5} \quad (psi) \quad (7-12)$$

If tensile strain ϵ_t is greater than the ultimate tensile strain (ϵ_{tu}), f_t is assumed to be equal to zero.

7.2.2 Material Modeling of Steel Strength

There are different numerical models to represent the stress-strain relationship of steel. The model employed for steel in this study is linearly elastic-perfectly plastic, as shown in Fig. 7-3. The complexity of this numerical model is located in the plastic portion of the model which does not include any strain hardening (perfectly plastic).

The elastic behavior of the steel is limited by the linearly elastic zone of this model at which the strain is less than the yield strain

$$\epsilon_y = \frac{f_y}{E_{so}} \quad (7-13)$$

where f_y is the yield stress of steel, and ϵ_y is the value of the steel strain at the end of the elastic zone where the stress is equal to f_y . E_{so} is the elastic Young's modulus of steel which is equal to 29,000 kips/inch².

When the value of steel stress (f_s) at any point on the cross section reaches the yield stress, the Young's modulus becomes less than E_{so} of the elastic zone. The initial yielding takes place when the stress at the farthest point from the neutral axis on the steel cross section (point A) becomes equal to the yield stress (f_y), as shown in Fig. 7-4a.

The initial yielding indicates the beginning of the elastic-plastic response of the steel section. By increasing the load, other internal points on the cross section will satisfy the yield stress to respond plastically under a constant yield stress (f_y), as seen in Figure 7-4b. Once all points on the steel section satisfy a normal stress (f_s) equal to the yield stress (f_y) or a strain value larger than the yield strain (ϵ_y), the steel section responds as a plastic hinge with an ultimate plastic moment (M_p) indicating the complete yielding of the steel section, as presented in Fig. 7-4c.

During the elastic-plastic stage (after the initial yielding and before complete yielding) some points on the steel section respond elastically ($f_s \leq f_y$) and the others respond plastically ($f_s = f_y$) with different values of Young's modulus (E_s), as presented in Fig. 7-3. The values of normal strain are assumed to vary linearly over the deformed cross section of steel.

If the strain at any point on the steel cross section is larger than the yield strain (ϵ_y), the plastic behavior will be governed by the flow of the steel under a constant stress (f_y) at the point in question. Regardless of whether the section is under elastic, elastic-plastic or plastic states, the strain is linearly distributed over the whole steel section. In addition, the strain at any point is controlled by the values of strain at other locations in order to keep the strain distribution linear. Generally, the external and internal moments over the steel section should be in a state of equilibrium.

7.3 MOMENT-CURVATURE (M-F) RELATIONSHIP

The aim of developing the moment-curvature relationship of the shaft material is to determine the variation of the flexural stiffness (EI) at every level of loading. The normal stress (σ_x) at any cross section along the shaft length is linked to the bending moment (M) and curvature (ϕ) by the following equations:

$$EI \frac{d^2 y}{d x^2} = M \quad (7-14)$$

$$EI \mathbf{f} = \frac{EI}{\mathbf{r}} = M \quad (7-15)$$

$$\mathbf{f} = \frac{d^2 y}{d x^2} = \frac{\mathbf{e}_x}{z} \quad (7-16)$$

$$\mathbf{e}_x = -\frac{z}{\mathbf{r}_o} \quad (7-17)$$

where

$$\mathbf{s}_x = E \mathbf{e}_x = E \mathbf{f} z \quad (7-18)$$

z = the distance from the neutral axis to the longitudinal fiber in question

ρ_o = the radius of curvature of the deflected axis of the shaft

ϵ_x = the normal strain at the fiber located z -distance from the neutral axis.

The above equations are based on the assumption of a linear variation of strain across the shaft cross section. In addition, the shaft cross section is assumed to remain perpendicular to the shaft axis before and after deforming, as shown in Fig. 7-5.

7.4 ANALYSIS PROCEDURE

The analysis procedure adopted consists of calculating the value of bending moment (M_i) at each cross section associated with a profile of the soil modulus of subgrade reaction which is induced by the applied load at the shaft top. Then, the associated curvature (ϕ), stiffness (EI), normal stress (σ_x) and normal strain (ϵ_x) can be obtained. This procedure depends on the shaft material. The profile of moment distribution

along the deflected portion of the shaft is modified in an iterative fashion along with the values of the strain, stress, bending stiffness and curvature to satisfy the equilibrium among the applied load and the associated responses of the soil and shaft. Based on the concepts of the SW model, the modulus of subgrade reaction (i.e. p-y curve) is influenced by the variations in the shaft bending stiffness at every shaft segment. This procedure guarantees the incorporation of soil-shaft interaction with the material modeling. The technique presented strives for a more realistic assessment of the shaft deflection pattern under lateral loading and due to the nonlinear response of shaft material and soil resistance.

7.4.1 Steel Shaft

Steel shafts involved in this study have circular cross sections, as seen in Fig. 7-6. The cross section of the steel shaft is divided into a number of horizontal strips (equal to a total of $2m$) parallel to the neutral axis. Each strip has a depth equal to the thickness of the pipe shaft skin, as seen in Fig. 7-7. The moment applied over the cross section of the shaft segment (i) is M_i , and the normal stress at a strip (n) is $(f_s)_n$ ($1 \leq n \leq m$).

Using Eqns. 7-17 and 7-18, the stress and strain distributions over the cross section of each shaft segment can be determined as

$$\mathbf{f}_i = \frac{M_i}{(EI)_i} \quad (7-19)$$

$$(\mathbf{e}_s)_n = z_n \mathbf{f}_i \quad 1 \leq n \leq m \quad (7-20)$$

$$(f_s)_n = (E_s)_n (\epsilon_s)_n \quad (7-21)$$

where $E_s \leq E_{s0}$; ϕ_i is the curvature at shaft segment (i) which is constant over the steel cross section at the current level of loading; z_n indicates the distance from the neutral axis to the midpoint of strip n; $(\epsilon_s)_n$ represents the strain at strip n; $(EI)_i$ represents the initial stiffness of the shaft segment (i); I is the moment of inertia of the steel cross section of the shaft segment (i) which is always constant; and E_{s0} symbolizes the elastic Young's modulus of the steel.

1. Elastic Stage

The Young's modulus of any strip of the steel section (i) is equal to the steel elastic modulus (29×10^6 psi) as long as the stress $(\epsilon_s)_n$ is less or equal to the yield strain. Consequently, there is no change in the stiffness value of the shaft segment (i) if ϵ_s at the outer strip ($n = 1$) is less than or equal to ϵ_y . This stage is similar to the linear analysis (constant EI) of the SW model presented in Chapter 5.

2. The Elastic-Plastic Stage

Once the calculated strain at the outer strip based on Eqn. 7-20 is larger than ϵ_y , the stress $(f_s)_n$ determined at the outer strip ($n = 1$) using Eqn. 7-21 will be equal to the yield stress. Therefore, initial yielding occurs and the elastic-plastic stage begins. During the elastic-plastic stage, the strips of the steel cross section experience a combination of elastic and plastic responses with different values of the secant Young's modulus (E_s). Some strips behave elastically ($\epsilon_s \leq \epsilon_y$ and $f_s \leq f_y$), and the others behave plastically ($\epsilon_s > \epsilon_y$ and $f_s = f_y$) with different values of the secant Young's modulus (E_s), as shown in Figs. 7-3, 7-4 and 7-8.

The normal stresses on the steel cross section are redistributed in order to generate a resisting moment $(M_R)_i$ that balances the applied moment (M_i) and satisfies the following equation:

$$M_i = (M_R)_i = (M_e)_i + (M_y)_i \quad (7-22)$$

where $(M_e)_i$ and $(M_y)_i$ represent the internal elastic and plastic moments induced over the steel cross section (i).

The internal elastic moment $(M_e)_i$ represents the internal moment exerted by the strips (m_1) which behave elastically and can be obtained as

$$(M_e)_i = \sum (f_s)_j A_j z_j \quad (1 \leq j \leq m_1) \quad (7-23)$$

The internal plastic moment $(M_y)_i$ is the moment generated by the yielded strips (m_2) which respond plastically and can be calculated using the following equation:

$$(M_y)_i = \sum f_y A_k z_k \quad (1 \leq k \leq m_2) \quad (7-24)$$

where A is the area of the steel strip, and

$$2 m = m_1 + m_2 \quad (4.25)$$

For the first iteration of the solution in this stage, the steel cross section experiences a resisting internal moment $(M_R)_i$ less than the external moment (M_i) . Therefore, the steel cross section of the shaft segment (i) should maintain a modified stiffness value for the shaft segment in question, i.e. $(EI)_{i,mod}$. This reduced value of stiffness at shaft segment (i) is associated with an increase in the value of curvature such that the

$$(f_i)_{mod} = f_i \frac{M_i}{(M_R)_i} \quad 7-13 \quad (7-26)$$

new value of curvature, $(\phi_i)_{\text{mod}}$, is

The modified stiffness value at shaft segment (i) can be computed using the following equation,

$$(EI)_{i,\text{mod}} = \frac{M_i}{(\mathbf{f}_i)_{\text{mod}}} \quad (7-27)$$

The above procedure should be performed with all the unbalanced segments along the deflected portion of the loaded shaft at each step of loading.

The global stability problem of the laterally loaded shaft is resolved under the same level of loading and soil resistance using the modified values of stiffness of the shaft segments (Eqn. 7-27). Consequently, the new moment distribution (M_i) along the shaft length is assessed during each iteration. The modification for shaft curvature and, therefore, stiffness values at the unbalanced segments continues until Eqn. 7-22 is satisfied over all the deflected segments of the shaft.

3. Plastic Stage

The elastic-plastic stage continues until the steel cross section reaches a condition of complete yield. Thereafter, all strips of the steel section will be subjected to the yield stress (f_y) and strain values larger than ϵ_y , as presented in Fig. 7-9. At this level of shaft head load, the steel section exhibits a plastic moment (M_p) which represents the ultimate moment that can be carried by the steel section. Once the steel section reaches the plastic moment, a plastic hinge develops to indicate the beginning of the plastic stage at the shaft segment in question. The plastic moment is expressed as

$$M_p = \sum f_y A_n z_n \quad (7-28)$$

Equations 7-26 and 7-27 are employed in order to obtain the desired values of curvature and the associated stiffness at the plastic section is

$$(EI)_{i,\text{mod}} = \frac{M_p}{(\mathbf{f}_i)_{\text{mod}}} \quad (7-29)$$

During the plastic stage, the moment capacity and the stress over the steel section are restricted to the plastic moment (M_p) and the yield stress (f_y), respectively. However, the strain and curvature values are free to increase in order to produce reduced stiffnesses with the higher level of loading.

The resisting moment of the completely yielded section (plastic hinge) is always equal to M_p . If the external moment (M_i) which is calculated from the global stability is larger than M_p , Eqns. 7-26, 7-28 and 7-29 will be employed. The iteration process continues until satisfying an external moment value equal to the plastic moment at the shaft segment in question.

The development of the plastic hinge on the shaft does not mean the failure of the shaft but leads to a limitation for the shaft-head load. After the formation of the plastic hinge, the shaft deflects at a higher rate producing larger curvatures and smaller stiffnesses to balance the applied load. Therefore, another plastic hinge may develop at another location on the shaft. If the soil has not failed at the development of the plastic hinge, the shaft may exhibit a lateral load capacity slightly larger than the load associated with the plastic hinge formation due to increase in soil resistance. The laterally loaded shaft is assumed to fail when the outer strip at any shaft segment experiences a strain value larger than 0.15.

7.4.2 Reinforced Concrete Shaft

The reinforced concrete shaft has a circular cross section and to be divided into a total number of horizontal

strips of (2m) as seen in Fig. 7-10. Unlike the cross section of a steel shaft, the cross section of the reinforced concrete shaft is not symmetrical around the neutral axis as a result of the different behavior of concrete under tensile and compressive stresses. The incorporation of concrete tensile strength reflects the actual response of the reinforced concrete shaft. As presented in Section 7.2.1, the employment of concrete confinement has a significant influence on the concrete behavior (strength and strain values).

The resistance of the concrete cover (outside the confined core of concrete) is neglected. Therefore, the initial stiffness of the whole concrete cross section $(EI)_i$ represents the effective concrete section which is the confined concrete core. The curvature (ϕ_i) at the concrete section (i) is initially determined based on the applied external moment M_i and the initial stiffness of the reinforced concrete cross section $(EI)_i$, i.e.

$$\mathbf{f}_i = \frac{M_i}{(EI)_i} \quad (7-30)$$

Based on a linear distribution of strain (ϵ) over the reinforced concrete cross section, the strain at any strip (n) can be obtained using Eqn. 7-20 and is expressed as

$$(\mathbf{e})_n = z_n \mathbf{f}_i \quad 1 \leq n \leq m \quad (7-31)$$

Eqns. 7-1 and 7-21, which represent the numerical models of the compressive stress of confined concrete and tensile stress of steel, respectively, are used to calculate the associated concrete stress (f_c) and steel stress (f_s) at each strip (n). In this study, the tensile stress (f_t) is assumed to be equal to the compressive stress (f_c) if the tensile strain $(\epsilon_t)_n$ is less than ϵ_{tu} , which is more conservative than Eqn. 7-10. Therefore, the reinforced concrete cross section remains symmetric (the centerline represents the neutral axis) as long as ϵ_t at the outer strip $(n = 1)$ is less than ϵ_{tu} . Under the conditions of a symmetric reinforced concrete section, the moment equilibrium and stiffness modification at any shaft segment (i) can be expressed as

$$(M_R)_i = \sum 2 [(f_c A_c)_n z_n + (f_s A_s)_n z_n] \quad (1 \leq n \leq m) \quad (7-32)$$

Once the value of the tensile strain at the outer strip of any shaft cross section exceeds ϵ_{tu} , the outer strip on the tension side fails and the cross section becomes unsymmetric. Thereafter, the neutral axis is shifted towards the compression side as shown in Fig. 7-10. In order to accurately estimate the new position of the neutral axis, the cross section should be in equilibrium under the compressive and tensile forces (F_{com} and F_{ten}) or

$$(F_{com})_i = (F_{ten})_i \quad (7-33)$$

where

$$(F_{com})_i = \sum (A_c f_c + A_s f_s)_n \quad 1 \leq n \leq n_1 \quad (7-34)$$

and

$$(F_{ten})_i = \sum (A_c f_t + A_s f_s)_n \quad 1 \leq n \leq n_2 \quad (7-35)$$

n_1 and n_2 are the numbers of strips in the compression and tension zones of the concrete cross section, respectively. At any strip in the tension zone, f_t is equal to zero when the tensile strain is greater than ϵ_{tu} .

Having the values of n_1 and n_2 ($2m = n_1 + n_2$) and using Eqns. 7-33 through 7-35, the location of the neutral axis can be identified, and the resisting moment can be determined as

where

$$(M_R)_i = (M_{com} + M_{ten})_i \quad (7-36)$$

$$(M_{com})_i = \sum [(f_c A_c + f_s A_s)_n (z_c)_n] \quad (1 \leq n \leq n_1) \quad (7-37)$$

$$(M_{ten})_i = \sum [(f_t A_c + f_s A_s)_n (z_t)_n] \quad (1 \leq n \leq n_2) \quad (7-38)$$

where z_c and z_t are the distance from the neutral axis to the strip in question in the compression and tension zones, respectively.

In addition, the behavior of steel bars in the compressive and tensile zones is subjected to the steel model presented in Section 7.2.2. Once the strain of any steel bar is greater than or equal to ϵ_y , f_s will be equal to f_y in Eqns. 7-34 through 7-38. The equations above are influenced by the ultimate values of concrete strength and strain (ϵ_{cu} and f_{cu}) that are associated with concrete confinement as presented in Section 7.2.1.

If the calculated moment $(M_R)_i$ is less than the external moment M_i , the cross section curvature will be modified to obtain new values for the curvature and stiffness to balance the applied moment, i.e.

$$(f_i)_{mod} = f_i \frac{M_i}{(M_R)_i} \quad (7-39)$$

The modified stiffness value at shaft segment (i) can be computed using the following equation,

$$(EI)_{i,\text{mod}} = \frac{M_i}{(\mathbf{f}_i)_{\text{mod}}} \quad (7-40)$$

By iteration, Eqns. 7-33 through 7-40 are employed to obtain the desired values of the curvature and the stiffness of the shaft segment (i) in order to generate a resisting moment $(M_R)_i$ equal to the external moment (M_i) . The above procedure should be performed with all unbalanced segments along the deflected portion of the loaded shaft at each level of loading.

The global stability problem of the laterally loaded shaft is solved again under the same level of loading and using the modified values of stiffness of the shaft segments. Consequently, the bending moment (M_i) is redistributed along the shaft length.

Once any concrete strip under compressive stress reaches the ultimate strain ϵ_{cu} (Eqn. 7-7), the strip fails and is excluded from the resisting moment. The steel bars fail when the steel strain reaches a value of 0.15. The strength of a failed strip is assumed to be equal to zero in Eqn. 7-28. However, the shaft fails when the stiffness of any shaft segment diminishes to a small value that does not provide equilibrium between the external and the resisting moments. Therefore, the plastic moment of a concrete shaft represents the largest induced moment in the shaft that can be sustained before failure.

7.4.3 Concrete Shaft with Steel Case (Cast in Steel Shell, CISS)

In the current case, the shaft cross section is treated as a composite section similar to the reinforced concrete shaft. The shaft cross section (steel and concrete) is divided into a number of strips (equal to $2m$) as shown in Fig. 7-9. The thickness of each strip is equal to the thickness of the steel shell (t_s). Both numerical material models presented in Section 7.2 are employed here using an iterative technique governed by the deformation criteria of the numerical models.

The normal strain is assumed to vary linearly over the shaft cross section which is perpendicular to the shaft

axis, as shown in Fig. 7-11. Therefore, the curvature is constant over the whole composite section. The applied bending moment (M_i) at shaft segment (i) generates initial values for curvature, stresses and strains in both the steel pipe and the concrete section as described in Section 4.2. Similar to the reinforced concrete section, the concrete resistance in the tension zone is considered. It should be noted that the steel pipe provides large concrete confinement resulting in large values of concrete strength and strain.

The composite cross section of shaft behaves symmetrically as long as the tensile strain at the outer strip of concrete ($n = 2$) is less than ϵ_{tu} . The strain values of steel and concrete are obtained using Eqns. 7-30 and 7-31. Then the associated stress values of concrete and steel are calculated based on Eqns. 7-1 and 7-21. Generally, the stiffness the composite cross section is modified according to the equilibrium between the external and internal moments as expressed by Eqn. 7-32 for the symmetric section.

When the tensile strain of the outer strip of concrete ($n = 2$) exceeds ϵ_{tu} , the composite cross section is no longer symmetric and the neutral axis location is shifted towards the compression zone and should be determined by using an iterative technique which includes Eqns. 7-36 through 7-39. It should be noted that the concrete tensile stress (f_t) at any failed strip in the tension zone is equal to zero. In addition, at any strip, the steel stress is equal to f_y if the strain is equal to or larger than ϵ_y . If the calculated resisting moment $(M_R)_i$ does not match the external moment (M_i), the stiffness of the shaft segment in question is modified using Eqn. 7-40.

The above procedure is performed with all shaft segments under the same level of loading. This procedure is repeated in an iterative way using the modified stiffness values to solve the problem of the laterally loaded shaft (global stability). The iteration process continues until there is equilibrium between the external and resisting moments at all shaft segments. The distribution of bending moment (M_i), along the length of the shaft, and the deflection pattern is based on the modified shaft stiffnesses and the resistance of the surrounding soil.

It should be noted that the concrete section will not fail before a plastic hinge develops. This occurs because the steel yields at a strain (ϵ_y) much less than the ultimate strain of concrete (ϵ_{cu}). However, the failed strips of concrete (in either the tension or compression zones) are subtracted from the composite section resulting in a faster drop in the stiffness of the shaft segment in question. It should be emphasized that there is no sudden failure for the concrete portion of the composite section because of the steel shell.

The stiffness of the loaded shaft and the effective area of the deflected shaft cross section vary according to the level of loading. Therefore, the actual moment-curvature relationship and the ultimate moment carried by a reinforced concrete shaft or a steel pipe shaft filled with concrete should be calculated using the technique presented.

7.4.4 Reinforced Concrete Shaft with Steel Case (Cast in Steel Shell, CISS)

Similar to the shaft cross section presented in Section 4.4.3, the shaft cross section is treated as a composite section. The shaft cross section (steel and reinforced concrete) is divided into a number of strips (equal to $2m$) as shown in Fig. 7-12. The thickness of each strip is equal to the combined thickness of the steel shell (t_s) and the thickness equivalent to the longitudinal reinforcement, A_s [$t_r = A_s / 3.14 / (Z_s - t_s)$]. Both numerical material models presented in Section 7.2 are employed here using an iterative technique governed by the deformation criteria of the numerical models.

The normal strain is assumed to vary linearly over the shaft cross section which is perpendicular to the shaft axis, as shown in Fig. 7-12. Therefore, the curvature is constant over the whole composite section. The applied bending moment (M_i) at shaft segment (i) generates initial values for curvature, stresses and strains in both the steel pipe and the concrete section as described in Section 7-2. The current shaft cross section (Fig. 7-12) is analyzed by following the procedure applied to the CISS section presented in Section 7.4.3.

7.5 SUMMARY

A technique for the inclusion of nonlinear material modeling for steel, concrete, and composite steel concrete

shafts has been developed and demonstrated in this chapter. The strain wedge model exhibits the capability of predicting the response of a laterally loaded shaft based on the nonlinear behavior of shaft material. The technique presented allows the designer to evaluate the location of a plastic hinge developed in the shaft, and to determine the realistic values of the ultimate capacity and the associated deflection of the loaded shaft.

The nonlinear behavior of the shaft material has an influence on the lateral response and capacity of the shaft/shaft. This effect is dependent on the values of bending moment (level of loading). In turn, the modulus of subgrade reaction (i.e. the p-y curve) is affected by the changed bending moment, the reduced bending stiffnesses, and the changed deflection pattern of the shaft/shaft. Without the appropriate implementation of material modeling, the shaft/shaft capacity, and the associated deflection pattern and bending moment distribution will be difficult to predict with any degree of certainty.

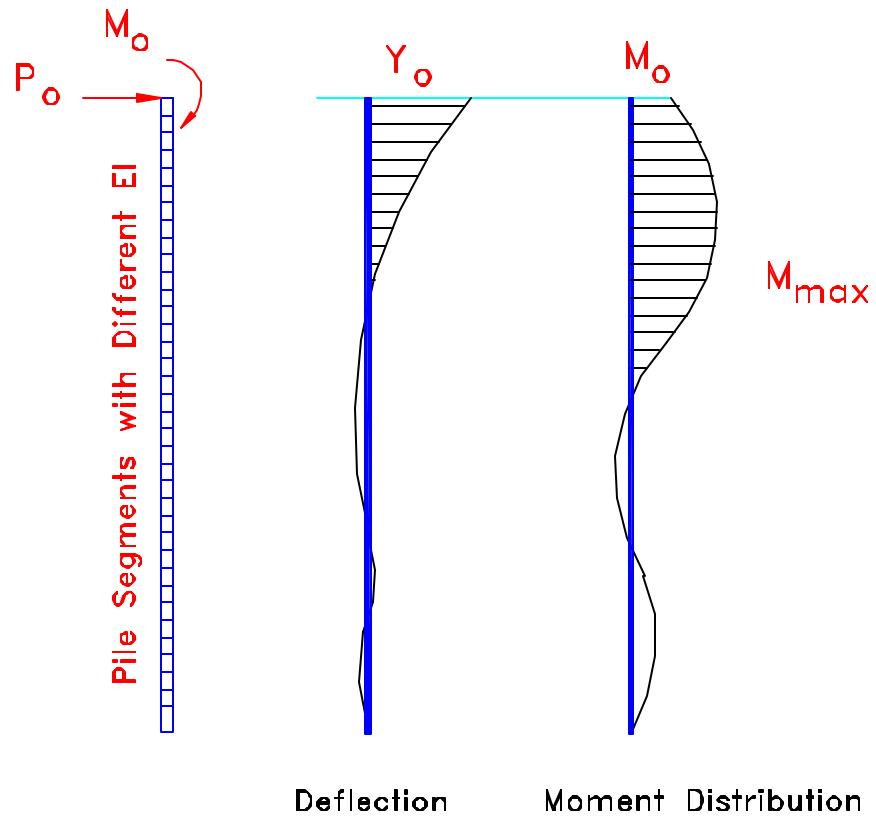


Fig. 7-1 Deflection and Moment Distributions in a Laterally Loaded Shaft

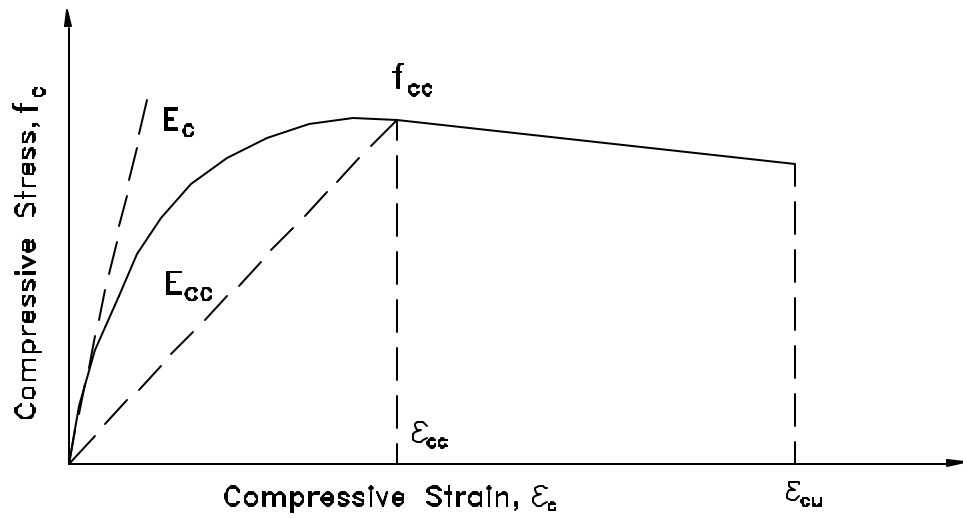


Fig. 7-2 Stress-Strain Model for Confined Concrete in Compression (Mander et al. 1984 and 1988)

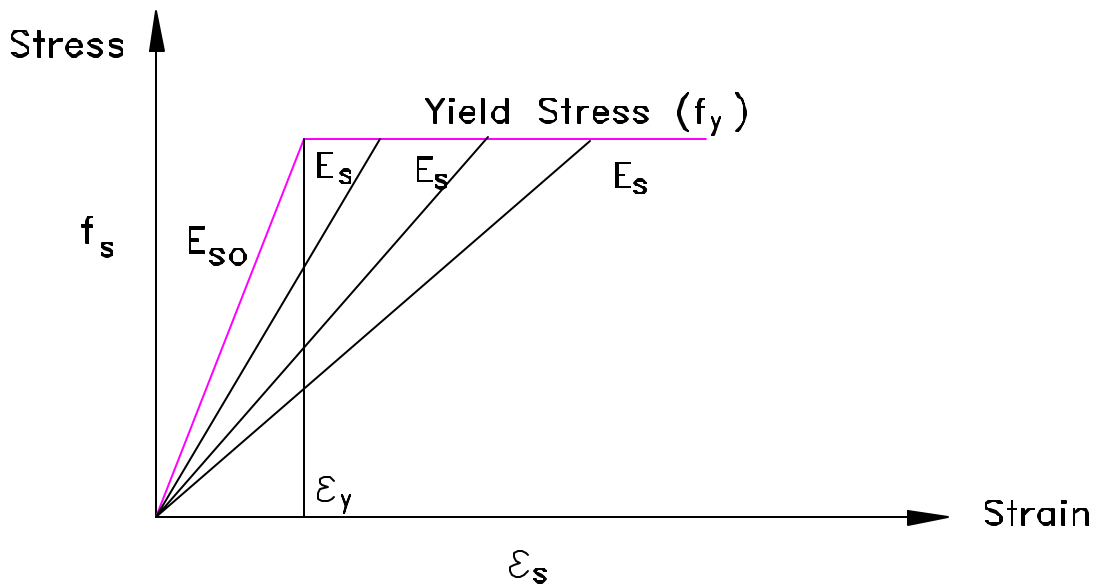


Fig. 7-3 Elastic-Plastic Numerical Model for Steel

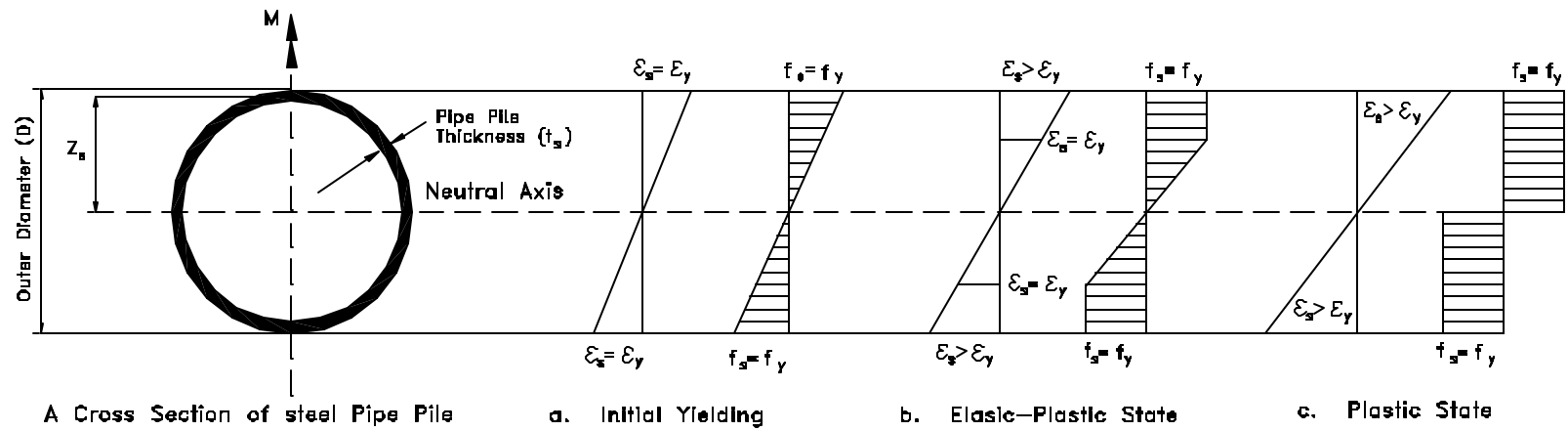
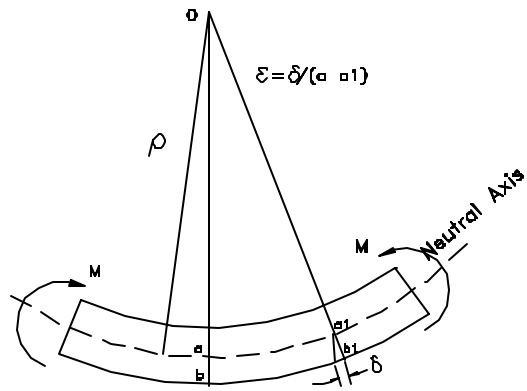
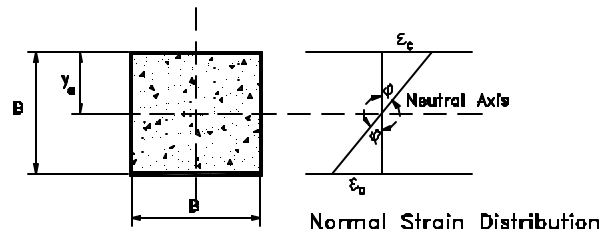


Fig. 7-4 Different stages of Normal Stresses over a Steel Section



A Pile Segment Subjected to bending Moment



A Cross section of a Concrete Pile Under Bending Moment

Fig. 7-5 Flexural Deformations of a Pile Segment subjected to Bending Moment

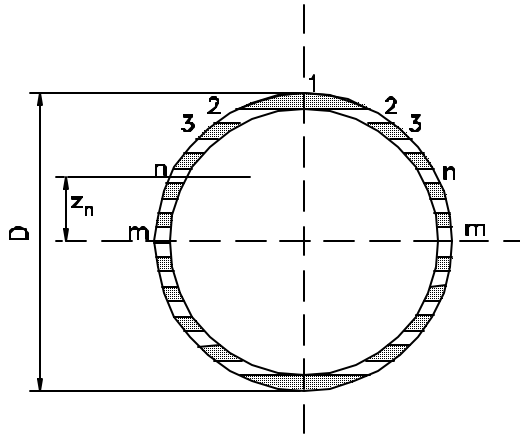


Fig. 7-6 A Cross Sections of Steel Shaft

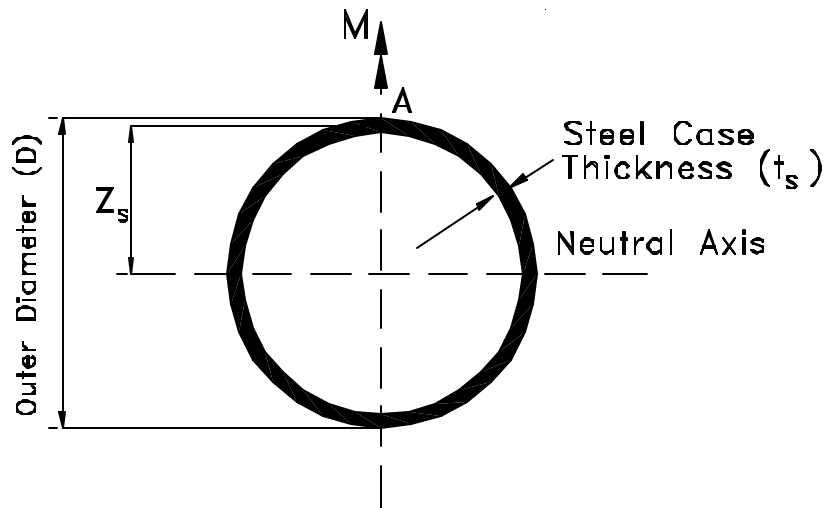


Fig. 7-7 Steel Sections Divided into Horizontal Strips

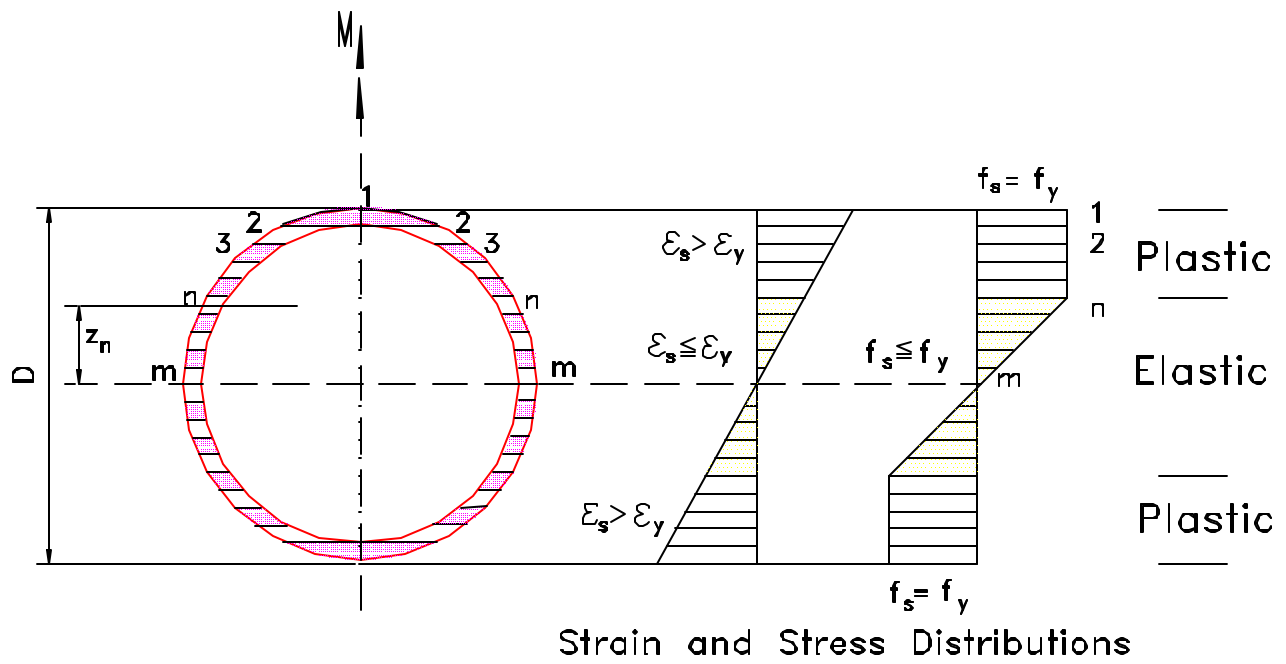


Fig. 7-8 Behavior of Steel Shaft Cross Section in the Elastic-Plastic Stage

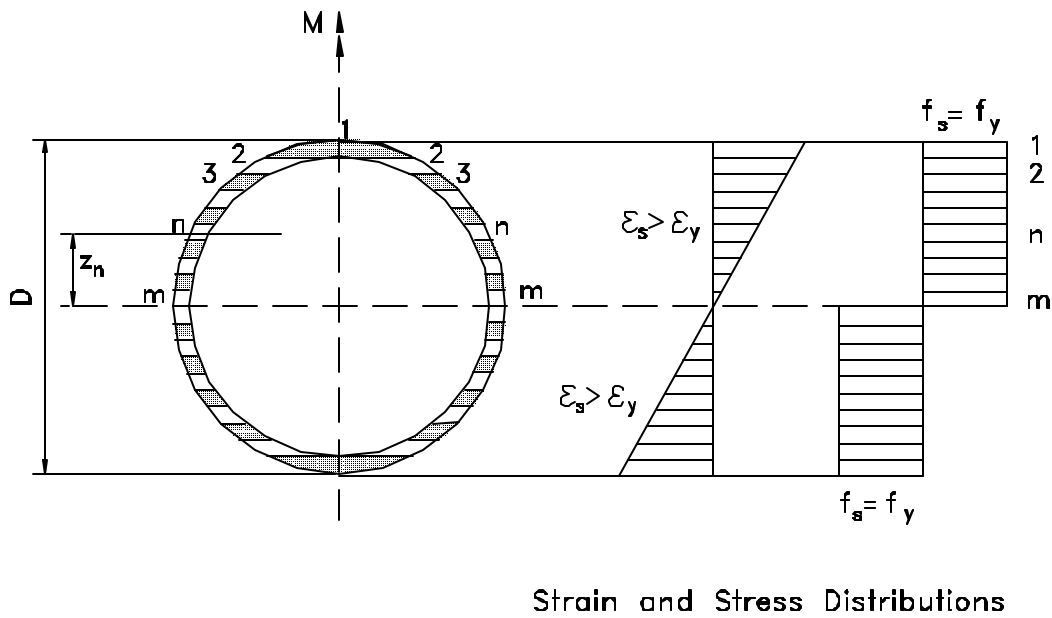
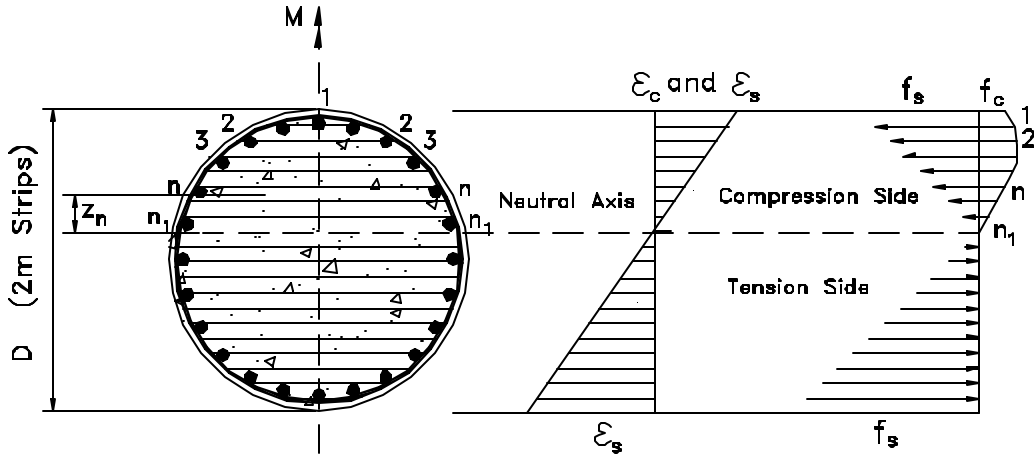
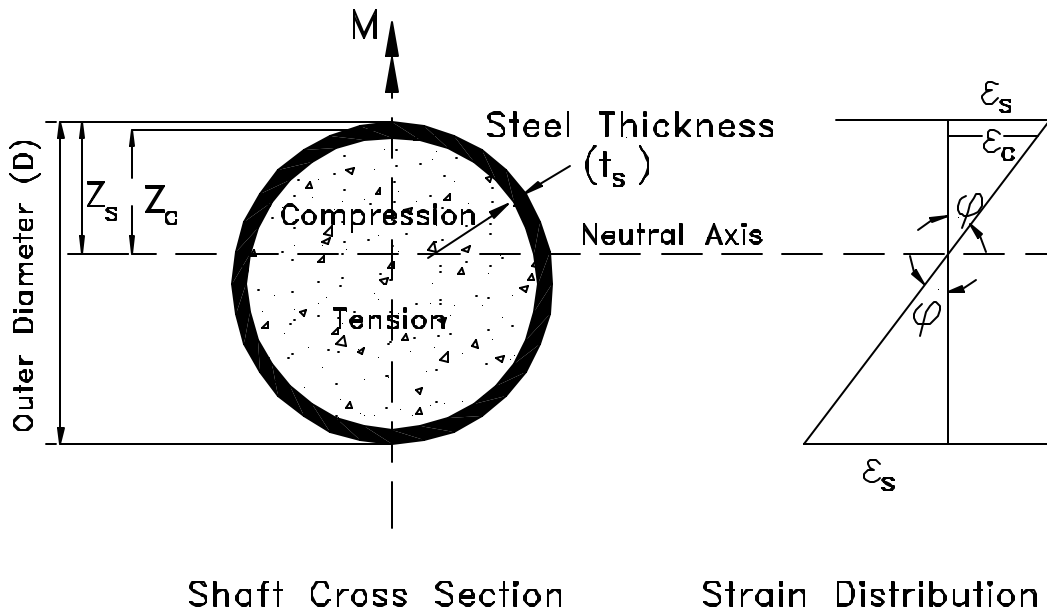


Fig. 7-9 Behavior of Steel Shaft Cross Section in the Plastic Stage



Strain and Stress Distributions

Fig. 7-10 Behavior of a Reinforced Concrete Shaft Cross Section Divided into Strips



Shaft Cross Section Strain Distribution

Fig. 7-11 Composite Cross Section of a Concrete Shaft with Steel Case (CISS)

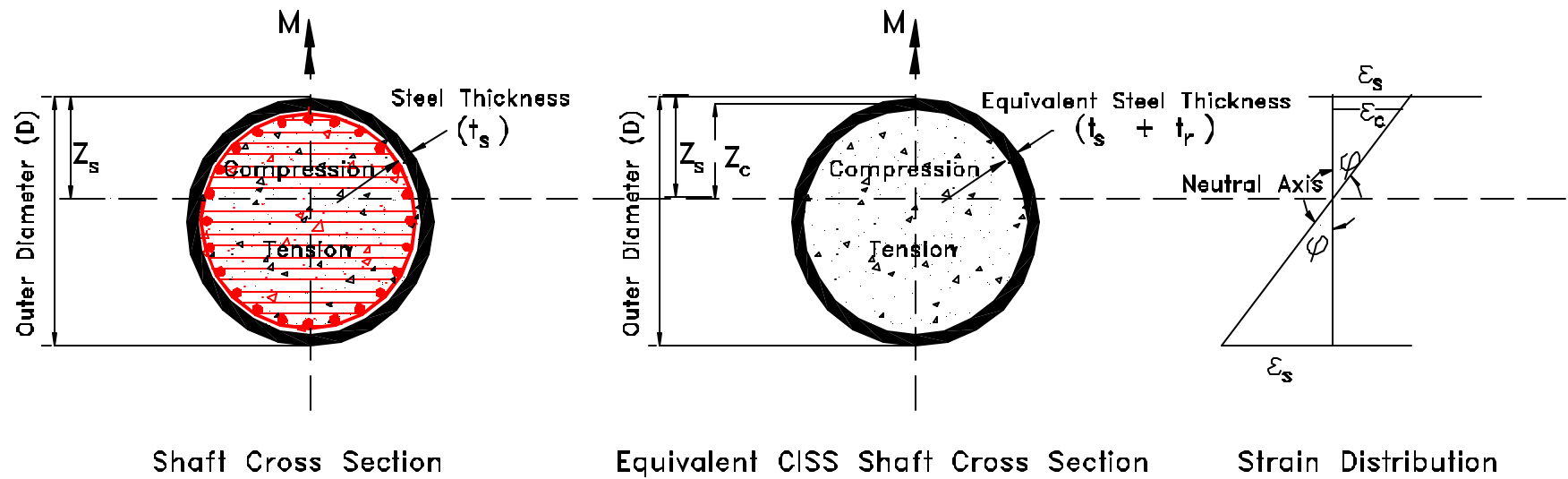


Fig. 7-12 A Shaft Cross Section of Reinforced Concrete Cast in Steel Shell